encit 2020

ABCM Associação Brasileira de Engenharia e Ciências Mecânicas

18th Brazilian Congress of Thermal Sciences and Engineering
November 16–20, 2020 (Online)

ENC-2020-0267
DEVELOPMENT AND VALIDATION OF A MONTE CARLO SOLVER COUPLED TO DIFFERENT SPECTRAL MODELS FOR RADIATIVE TRANSFER IN PARTICIPATING MEDIA

Guilherme Crivelli Fraga
Francis Henrique Ramos França
Federal University of Rio Grande do Sul, Mechanical Engineering Department - 425 Sarmento Leite St., Porto Alegre, RS Brazil
guilhermecfraga@gmail.com
frfranca@mecanica.ufrgs.br

Abstract. *The implementation of the Monte Carlo (MC) method for the radiative transfer in a one-dimensional medium slab is reported and validated through comparisons with an in-house, discrete ordinates method (DOM)-based code, as part of an ongoing research on the application of MC methods in radiative transfer problems. The method is implemented as a Fortran code and is capable for solving the radiative transfer problem for homogeneous and non-homogeneous media subjected to isothermal or non-isothermal conditions and bounded by black or gray walls. Three widely used spectral models are coupled to the MC solver: the gray gas (GG), the weighted-sum-of-gray gases (WSGG), and the spectral line-based WSGG models (SLW). The comparisons with the DOM solution are carried out for a set of test cases, and show a remarkable agreement for the two solutions regardless of the spectral model employed, attesting that the MC method was implemented successfully.*

Keywords: *Thermal radiation, Monte Carlo method, gray gas model, weighted-sum-of-gray-gases model, one-dimensional medium*

1. INTRODUCTION

Thermal radiation from participating media plays an important role in many high-temperature applications, such as in furnaces, fires and other types of combustion systems. Among the models for solving the radiation field, the Monte Carlo (MC) method is a versatile technique that may be applied to problems with varied degrees of complexity with relative ease (Modest, 2013). Differently from radiation models that aim to directly solve the radiative transfer equation (RTE), often through a finite difference of finite volume approach, the MC method relies on sampling a very large number of bundles of photons emitted at various points throughout the medium, and tracking their individual paths of until they are absorbed.

Monte Carlo methods can be applied to virtually any mathematical problem that can be solved by a statistical sampling technique. Its first usage in the thermal radiation field was in the 1960s by Fleck, 1961, Howell and Perlmutter, 1964a,b, and Perlmutter and Howell, 1964, and it has since been widely used for solving the radiative exchange between surfaces and radiative transfer problems in participating media (Howell, 1998; Haji-Sheikh and Howell, 2006). Moreover, variations of the standard MC method have arisen, like the reverse Monte Carlo (Howell *et al.*, 2016), that is more efficient for problems, such as determining the intensity incident across a small cone of angles at a specific region of a large domain; the energy-partitioning MC (Modest and Poon, 1961; Modest, 1978), which significantly reduces the computational costs of the standard MC method for optically thick media; and the direct exchange MC (Cherkaoui *et al.*, 1996, 1998), adequate for near-isothermal enclosures.

The versatility of the MC method has also allowed it to be combined to other techniques, further enhancing its accuracy and the range of problems for which it can be applied. Examples of this include its coupling to the line-by-line method, first reported by Tang and Brewster, 1999, and Wang and Modest, 2007b, and its adaptation for media represented by discrete particle fields (Wang and Modest, 2006, 2007a), which models the interaction between the infinitesimally thin photon rays of the MC method and the infinitesimal point-masses that are employed in the modeling of turbulent combustion using stochastic probability density functions.

The work reported in this text is the initial part of an ongoing research on the application of MC methods in radiative transfer problems. In this framework, this study presents the development of a Monte Carlo solver for computing the one-dimensional radiative transfer in participating media bounded by black or gray walls. The method has been applied alongside different spectral models for the wavenumber dependence of the radiative properties of participating media—namely, the gray gas (GG), weighted-sum-of-gray-gases (WSGG) and spectral line-based WSGG (SLW) models. To validate the constructed solver, comparisons to a well-established in-house code are carried out for a set of cases

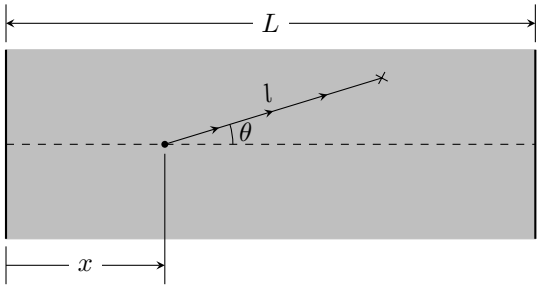

Figure 1. Schematic representation of the one-dimensional domain under study, with the illustration of a bundle being emitted at position x (black circle) and absorbed after traveling a length l (black cross)

involving homogeneous and non-homogeneous carbon dioxide and water vapor mixtures at isothermal and non-isothermal conditions.

2. THE MONTE CARLO METHOD

The Monte Carlo method as adopted in the present study consists of sampling a large number of discrete bundles of radiative energy and following their individual paths until they are absorbed in the system. These paths are determined at each point of emission and reflection by a random choice from the set of possible paths. Similarly, the position at which any given bundle is emitted is also determined in a random fashion, and the energy associated to the bundle is related to the local radiative emission and to the total number of bundles that are emitted at that position. By tracking the paths of all bundles, the net radiation loss at any arbitrary point within the medium may be calculated as the difference between the total local emission and the sum of the energy of all bundles that are absorbed at that point. Proceeding in this manner, very accurate results can be obtained as long as a sufficiently large number of bundles are sampled (Howell and Perlmutter, 1964a).

Consider the radiative transfer problem in a one-dimensional medium slab of total width L bounded by two parallel gray walls, as illustrated in Fig. 1. Denote first the radiative emission (per unit volume) at a given position x within the medium as $\dot{Q}^m_{emi,x} = 4\sigma\kappa_P T^4$, where σ is the Stefan-Boltzmann constant, and κ_P and T are the Planck-mean absorption coefficient and the temperature at x, respectively. Then, the probability that a bundle is emitted at position x within the medium may be defined as (Modest, 2013)

$$R^m_x = \frac{\int_0^x \dot{Q}^m_{emi,x'}\,\mathrm{d}x'}{\int_0^L \dot{Q}^m_{emi,x'}\,\mathrm{d}x'} = \frac{1}{Q^m_{emi}}\int_0^x \dot{Q}^m_{emi,x'}\,\mathrm{d}x' \,, \tag{1}$$

where x' is a generic variable for integration and Q^m_{emi} is the medium-integrated radiative emission. Equation (1) can be readily inverted to express x in terms of R^m_x, so that the choice of any R^m_x between 0 and 1 yields a unique value of x.

In a scenario where the walls that bound the medium are at a non-zero temperature, they are also expected to emit a portion of the overall energy bundles, and, as a consequence, to affect the number of bundles that is emitted at any given position within the medium. To account for this, start by denoting the radiative emission from the left and right walls (w_1 and w_2) as $Q^{w_1}_{emi} = \varepsilon_{w_1}\sigma T^4_{w_1}$ and $Q^{w_2}_{emi} = \varepsilon_{w_2}\sigma T^4_{w_2}$, where ε_{w_1} and ε_{w_2} are the total hemispherical emissivities of the walls and T_{w_1} and T_{w_2} are their temperature, respectively. In this manner, the total radiative energy that is emitted by the medium and by the walls is $Q_{emi} = Q^{w_1}_{emi} + Q^m_{emi} + Q^{w_2}_{emi}$ (notice that the superscript $(\cdot)^m$ in Q^m_{emi} and in Eq. (1) indicate that the quantities are evaluated for the medium alone), and the probability that the bundle is emitted by either one of the walls or by the medium at position x is given by

$$R_x = \frac{1}{Q_{emi}}\left[Q^{w_1}_{emi} + \int_0^x \dot{Q}_{emi,x'}\,\mathrm{d}x' + Q^{w_1}_{emi}\delta(x-L)\right]. \tag{2}$$

where δ is the Dirac delta function. The above equation is written in such a way that R_x is still bounded between 0 and 1, with the left wall (i.e., $x = 0$) emitting a bundle whenever $R_x \leq Q^{w_1}_{emi}/Q_{emi}$, and the right wall ($x = L$), whenever $R_x \geq (Q^{w_1}_{emi} + Q^m_{emi})/Q_{emi}$; otherwise, the bundle is emitted within the medium, and its position x can be found by inverting Eq. (2) and solving for x.

In an analogous manner to how Eq. (1) was derived, it is possible to show that the probability that a bundle in the medium be emitted along the direction characterized by the polar angle θ is given as (Modest, 2013)

$$R^m_\theta = \frac{\int_0^\theta \sin\theta'\,\mathrm{d}\theta}{\int_0^\pi \sin\theta'\,\mathrm{d}\theta} = \frac{1}{2}(1-\cos\theta)\,. \tag{3}$$

Therefore, a single angle of emission θ can be obtained for any $0 \leq R_\theta \leq 1$. It should be mentioned that Eq. (3) is only valid for relating θ to R_θ^m within the medium (notice again the m superscript), and the integral in that equation is more complex for the direction of bundles emitted or reflected by a solid wall. In the present study, the walls that bound the medium are assumed to be diffuse, in which case the probability that a bundle is emitted or reflected along direction θ is (Modest, 2013)

$$R_\theta^w = \frac{\int_0^\theta \sin\theta' \cos\theta' \, \mathrm{d}\theta}{\int_0^{\pi/2} \sin\theta' \cos\theta' \, \mathrm{d}\theta} = \sin^2\theta \,, \tag{4}$$

where the $(\cdot)^w$ superscript has been included in the left-hand side to evidence that the probability refers to an event that occurs at one of the walls.

Once an energy bundle hits one of the domain's walls, it can be absorbed or reflected back into the medium. The probability of the bundle being absorbed is directly related to the absortivity α_w of wall w: if $R_\alpha \leq \alpha_w$, then the bundle is absorbed, and the bundle's energy is tallied to the total energy absorbed by that wall; otherwise, it conserves its energy and is reflected into the medium, at a direction determined following the probability expressed by Eq. (4). Also, because the walls in the present study are either black ($\alpha_w = 1$ and all incident bundles are absorbed) or gray, the wall's absorptivity are equal to its emissivity, ε_w, so that the condition for a bundle to be absorbed by wall w can be stated as $R_\alpha \leq \varepsilon_w$

2.1 The gray gas (GG) model

The GG model assumes that the absorption coefficient of the medium does not vary across the radiation spectrum Howell *et al.* (2016). Hence, $\kappa_P = \kappa$ and $\dot{Q}^m_{emi,x} = 4\sigma\kappa T^4$ (note that κ can depend on the local temperature, pressure and medium composition, so that some care is still needed when carrying out the spatial integration in Eq. (2)). Furthermore, the fraction of energy penetrating through a layer of medium of length l is then $\exp\left(-\int_0^l \kappa \, \mathrm{d}l'\right)$, so the following can be defined (Modest, 2013):

$$R_l = \exp\left(-\int_0^l \kappa \, \mathrm{d}l'\right), \tag{5}$$

with R_l the probability that a bundle travels a distance l until being absorbed by the medium.

2.2 The weighted-sum-of-gray-gases (WSGG) model

In the WSGG model, the non-gray absorption spectrum is represented as a combination of a small number J of gray gases j, each with an absorption coefficient κ_j that does not vary with the wavenumber. A detailed discussion on the assumptions behind the WSGG model and its limitations is provided elsewhere (see, e.g.,Modest, 1991). For the purposes of this paper, suffice it to say that the Planck-mean absorption coefficient in the framework of this model is given as $\kappa_P = \sum_{j=1}^J \kappa_j a_j$, where a_j is the fraction of blackbody energy corresponding to gas j, usually modeled as a simple polynomial function of the local temperature.

Rather than its energy being distributed across the entire radiation spectrum, as it was for the previous exposition on the GG model, a bundle now will be emitted within the spectral intervals that correspond to one gray gas j only, which in a MC method should also be chosen randomly. How to express the probability that a bundle be emitted by gas j depends on whether this bundle is emitted by the medium or the wall. For the former, such probability can be defined as the ratio between the cumulative radiative emission (per unit volume) of all gases $j' \leq j$ at position x and the total radiative emission at that position, or

$$R_J^m = \frac{\sum_{j'=1}^j 4\sigma\kappa_{j'} a_{j'} T^4}{\sum_{j'=1}^J 4\sigma\kappa_{j'} a_{j'} T^4} = \frac{1}{\kappa_P} \sum_{j'=1}^j \kappa_{j'} a_{j'} \,. \tag{6}$$

For the walls, a similar expression is used, but now considering the energy emitted by a solid boundary (per unit area)

$$R_J^w = \frac{\sum_{j'=0}^j \varepsilon_w a_{j'} \sigma T^4}{\sum_{j'=0}^J \varepsilon_w a_{j'} \sigma T^4} = \sum_{j'=0}^j a_{j'} \,. \tag{7}$$

A few comments should be made regarding these equations. First, note that R_J^m and R_J^w have stepwise variations within the 0 to 1 interval, as opposite to all probabilities defined previously (with the exception of R_x^m). Therefore, if for instance Eq. (6) is inverted, any value of $\sum_{j'=1}^j \kappa_{j'} a_{j'}/\kappa_P \leq R_J^m < \sum_{j'=1}^{j+1} \kappa_{j'} a_{j'}/\kappa_P$ will correspond to a bundle being emitted by gas j. Second, the lower j bound of the summation in Eq. (7) is $j = 0$; this corresponds to the spectral windows where the

gas is transparent to thermal radiation (i.e., $\kappa_0 = 0$), for which the a_j coefficient is computed as $a_0 = 1 - \sum_{j=1}^{J} a_j$. For the gray gases themselves, κ_j and a_j can be determined from the local thermodynamic state by choosing an appropriate set of correlations. In this study, the formulation of Dorigon *et al.*, 2013 is used for this purpose, in which these coefficients are given as

$$\kappa_j = \kappa_{pj} p_a \,; \qquad a_j = \sum_{k=0}^{4} b_{j,k} T^k \,, \tag{8}$$

where p_a is the partial pressure of the participating mixture, and the gray gas pressure-based absorption coefficient κ_{pj} and polynomial terms $b_{j,k}$ are constant coefficients whose values depend on the gray gas index. For more information on this formulation of the WSGG model, the reader is referred to the original paper by Dorigon *et al.*, 2013.

Finally, the probability that an energy bundle is absorbed at length l in the WSGG model depends on the absorption coefficient of the gray gas that the bundle belongs to. Therefore, Eq. (5) becomes

$$R_l = \exp\left(-\int_0^l \kappa_j \, \mathrm{d}l'\right). \tag{9}$$

2.3 The spectral line-based WSGG (SLW) model

The SLW model is an evolution of the WSGG model reported to be more accurate in many scenarios (Webb *et al.*, 2019). Its core formulation is similar to that of the WSGG model, with the absorption spectrum divided into a set of J gray gases spread in a non-contiguous fashion, to which an absorption coefficient κ_j and a weighting coefficient a_j are assigned. Therefore, for the purposes of implementing a MC method, the selection of which gray gas emits a given energy bundle still follows Eqs. (6) and (7), and the distance l traveled by this bundle until it is absorbed is also determined from Eq. (9).

The differences between the WSGG and SLW models arise in the way that the κ_j and a_j coefficients are determined. Rather than using a predefined correlation for calculations of these parameters, the SLW model introduces the concept of an absorption line blackbody distribution function (ALBDF). For a thermodynamic state ϕ and at a source temperature T_b, the ALBDF F is given as (Denison and Webb, 1993)

$$F(C, \phi, T_b) = \int_{C_\eta(\phi)<C} \frac{I_{b\eta}(T_b)}{I_b(T_b)} \, \mathrm{d}\eta \,, \tag{10}$$

where $C_\eta(\phi)$ is the gas absorption cross-section at thermodynamic state ϕ, $I_{b\eta}(T_b)$ is the Planck function or spectral blackbody intensity evaluated at $T = T_b$, and $I_b(T_b) = \int_0^\infty I_{b\eta}(T_b) \, \mathrm{d}\eta$. The absorption cross-section is related to the spectral absorption coefficient κ_η of the gas as $\kappa_\eta = N X_a C_\eta$, in which N is the gas molar density and X_a is the mole fraction of the gas.

According to Eq. (10), the ALBDF gives the fraction of the total blackbody intensity at source temperature T_b in the portions of the spectrum for which the gas absorption cross-section at a thermodynamic state ϕ is below a given value C. As such, the a_j coefficient can be determined as

$$a_j = F(\tilde{C}_j, \phi, T_b) - F(\tilde{C}_{j-1}, \phi, T_b) \tag{11}$$

for two successive supplementar cross-sections $\tilde{C}_{j-1}$ and $\tilde{C}_j$. On the other hand, the gray gas absorption coefficient is calculated from the gray gas absorption cross-sections C_j as

$$\kappa_j = N X_a C_j \,, \tag{12}$$

where C_j is typically determined as the geometric mean of two successive supplementar cross-sections, $C_j = \sqrt{\tilde{C}_j \tilde{C}_{j-1}}$.

The application of the SLW model is straightforward if the medium is composed by a single participating species at homogeneous and isothermal conditions, but some additional care is needed if that is not the case. Because the ALBDFs are not expected to be the same for the individual species, a method must be devised for dealing with mixtures. Furthermore, if the medium is not at a homogeneous and isothermal condition, the supplementar cross-sections may vary throughout the optical path as the thermodynamic state changes. Different formulations of the SLW can then be achieved by selecting between one of the many ways that have been devised for solving these issues. In the present study, the multiplication approach (Solovjov and Webb, 2000) is adopted for modeling the gaseous mixture, and the rank-correlated method (Solovjov *et al.*, 2018b) is used for applying the SLW model to non-uniform media. However, note that the MC solver implemented in this study has also been validated for many other SLW formulations.

2.4 Methodology of solution

From the previous definitions, the solution of the radiative transfer problem with the MC method is as follows: first, a large number N_b of bundles is selected and the computational domain is divided into N_c cells, each cell i with width δx_i. In the present study, the cells are uniformly spaced, so $\delta x_i = \delta x = L/N_c$. Then, a random number R_x^m between 0 and 1 is assigned to each bundle to define its position of emission by inverting Eq. (2); this position can be translated into a grid point by expressing the integral in that equation as a quadrature, $\int_0^x \dot{Q}^m_{emi,x'}\,\mathrm{d}x' = \sum_{i'=1}^{i} \dot{Q}^m_{emi,i'}\delta_{x,i'}$, where $\dot{Q}^m_{emi,i} = 4\sigma\kappa_{P,i}T_i^4$ is the radiative emission computed at grid point i. Once all N_b bundles are tallied, each grid cell i will emit a total of $N_{b,i}$ of bundles, from which the energy of each bundle emitted by the cell can be determined simply as $Q^m_{emi,b,i} = \dot{Q}^m_{emi,i}\delta x_i/N_{b,i}$ (where it is assumed that all bundles emitted by the same cell have the same energy). Similarly, the energy of each bundle emitted by one of the walls is given as $Q^{w_i}_{emi,b} = \dot{Q}^{w_i}_{emi}/N_{b,w_i}$ for $w_i = 1$ or 2, where N_{b,w_i} is the number of bundles emitted by the wall.

Afterwards, to each bundle another set of two random numbers are assigned: R^m_θ or R^w_θ (depending on whether the bundle is emitted by a cell within the medium or by one of the walls), from which the direction along which the bundle will travel is determined, and R_l, which defines the distance that the bundle travels until it is absorbed. For the WSGG and SLW models, a third random number is also generated, R^m_J or R^w_J, to define to which gray gas does the bundle belong. In the same way as the spatial integration in Eq. (2), the integration in Eq. (5) or Eq. (9) is also replaced by a quadrature, with κ (or κ_j) assumed to be constant within each grid cell. Once the length l until absorption is defined, the grid cell where the bundle is absorbed is known, and the energy of the bundle can be added to the total energy absorbed at that position. If, however, l is larger than the distance from the emitting cell until the wall (note that this distance depends on the position where the bundle was emitted and on the angle of emission θ), then the bundle will hit the wall and can be either absorbed or reflected; a new random number R_α is generated to define this, as previous discussed. For any reflected bundle, new R^w_θ and R_l are assigned to determine their direction and length until absorption.

After all bundles have been absorbed, the local net radiation loss in the medium (per unit volume) is calculated as $\dot{Q}^m_{net,i} = \dot{Q}^m_{emi,i} - Q^m_{abs,i}/\delta x_i$, where $Q^m_{abs,i}$ is the sum of the energies of all bundles that are absorbed at grid cell i. Furthermore, recognizing that the net radiation loss is given by the gradient of the local radiative heat flux q^m, or $\dot{Q}^m_{net} = \mathrm{d}q^m/\mathrm{d}x$ for the one-dimensional medium under study, the radiative heat flux at cell i can be approximated as $q^m_i = q^m_{i-1} + \dot{Q}^m_{net}\delta x_i$. Finally, the radiative heat flux on the walls is obtained by a simple energy balance, $q_{w_i} = \varepsilon_{w_i}\sigma T^4_{w_i} - Q^{w_i}_{abs}$, with $Q^{w_i}_{abs}$ the tally of the energy of the bundles that are absorbed at wall w_i.

3. RESULTS AND DISCUSSION

The MC method described in the previous sections has been implemented as a Fortran code for the solution of the radiative transfer problem in a one-dimensional medium slab subjected to uniform or non-uniform temperature and species concentration fields. The validation of such implementation is presented next.

For this purpose, four benchmark cases are studied here, characterized by two different temperature and medium composition profiles and by two sets of wall emissivities. For all cases, the walls that bound the medium are cold (relative to the medium temperature), kept at a temperature $T_w = 400\,\mathrm{K}$. A isothermal and a non-isothermal temperature distribution are considered; in the former, the temperature of the medium is set to $T = 1100\,\mathrm{K}$, and, in the latter, it follows the symmetrical spatial profile

$$T(x^\star) = 400\,\mathrm{K} + 1400\,\mathrm{K}\sin^2\left(\pi x^\star\right), \tag{13}$$

where $x^\star = x/L$. The medium is a mixture water vapor, carbon dioxide and a transparent species, either with a homogeneous composition (with the molar fractions of H_2O and CO_2 $X_w = 0.2$ and $X_c = 0.1$, respectively) or with the following non-homogeneous profiles:

$$X_w(x^\star) = 0.2\sin^2\left(\pi x^\star\right); \qquad X_c = X_w/2\,. \tag{14}$$

The four cases are obtained by combining these profiles for two conditions: black walls ($\varepsilon_{w_1} = \varepsilon_{w_2} = 1.0$) and gray walls with different emissivities ($\varepsilon_{w_1} = 0.2$ and $\varepsilon_{w_2} = 0.8$). Table 1 gives an overview of the parameters of each case and their denominations. For all of them, the medium is subjected to a total pressure of 1 atm and the distance between the two bounding walls is $L = 1\,\mathrm{m}$.

The reference to which the results of the MC method are compared is provided by a finite differencing solution of the RTE using the discrete ordinates method (DOM), with the set of quadrature and weights of Lathrop and Carlson, 1964, for a total of twenty ordinates. The spatial grid for this solution consists of $N_c = 400$ uniformly-spaced cells (the same number of cells is also used for the MC method). The DOM solution with the GG, WSGG and SLW models is carried out in an in-house Fortran-based code that has already been validated and used in a number of previous studies (e.g., Fonseca *et al.*, 2018, and Fraga *et al.*, 2019), so it can be safely regarded as the benchmark solution.

Table 1. Test cases considered to evaluate the MC method implementation. In all cases, $X_c = X_w/2$

	T profile	X_w profile	ε_{w_1}	ε_{w_2}
Case 1.b	1100 K	0.2	1.0	1.0
Case 1.g	1100 K	0.2	0.2	0.8
Case 2.b	Eq. (13)	Eq. (14)	1.0	1.0
Case 2.g	Eq. (13)	Eq. (14)	0.2	0.8

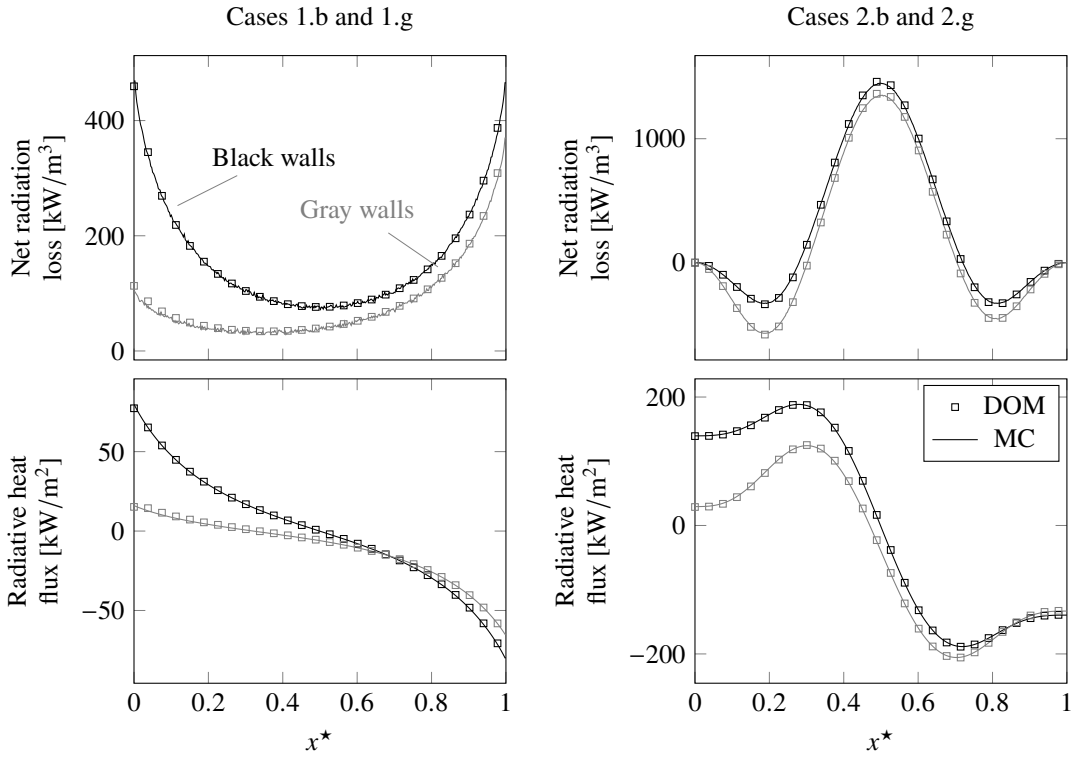

Figure 2. Comparison between the results of the DOM and of the MC method for the GG model

3.1 The MC-GG solution

Figure 2 reports the spatial distributions of the net radiation loss and the radiative heat flux calculated for the four cases in Table 1 using the GG model for the spectral treatment of the radiative exchange. For the application of this model, the correlations of Cassol *et al.*, 2015, are used to determine the absorption coefficient κ of the gray medium. A total of $N_b = 10^8$ bundles has been employed for each MC solution; the justification for employing such great number of bundles is that the isothermal cases (1.1b and 1.1g) require a large quantity of bundles to be emitted at all grid cells for a statistically significant solution. Even so, it is still possible to see in Fig. 2 some oscillations of the resulting profiles for the net radiation loss obtained by the MC method; the results for Cases 2.b and 2.g, on the other hand, show no visible oscillation. The sensibility of the present results to the total number of bundles is further discussed in Section 3.4.

The agreement between the DOM and MC solutions is evident for all cases. For instance, the relative difference between the two solutions for the radiative heat flux at the walls for Cases 1.b and 1.g is around 3.0 %, and for the radiation loss at $x^\star = 0.5$ (the point of maximum radiation loss) for Cases 2.b and 2.g it does not surpass 1.5 %. Considering that the DOM itself does not provide an exact solution to the radiative transfer problem, but only an approximation of it, this level of error is deemed acceptable.

3.2 The MC-WSGG solution

Results of the DOM and MC solutions with the WSGG model for the net radiation loss and radiative heat flux are depicted in Fig. 3. As noted in Section 2.2, the WSGG correlations of Dorigon *et al.*, 2013, have been used for these calculations, and once again the total number of bundles is set to $N_b = 10^8$, for the same reason given in Section 3.1. The agreement of the MC method to the DOM is again very good. In fact, it is even better than for the GG model, with the relative differences between the two solutions for the radiative heat flux at the walls below 2.0 % (Cases 1.b and 1.g), and

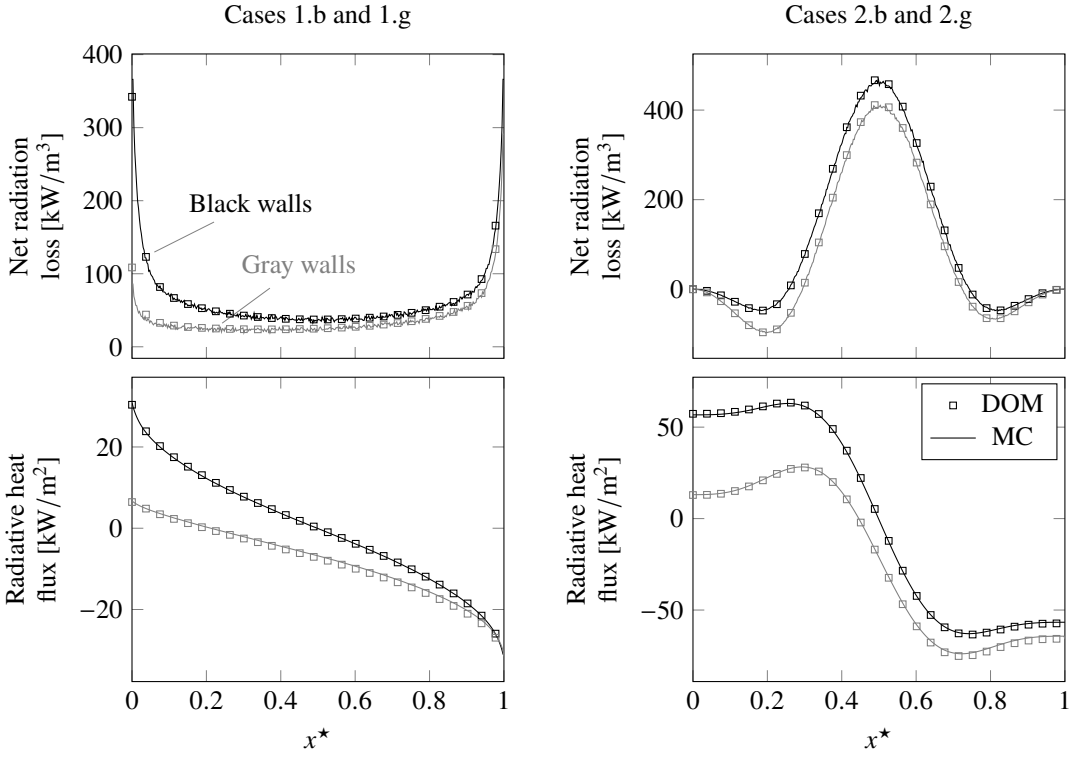

Figure 3. Comparison between the results of the DOM and of the MC method for the WSGG model

for the radiation loss at $x^\star = 0.5$, below 1.0 % (Cases 2.b and 2.g).

3.3 The MC-SLW solution

Figure 4 plots the results for the radiation loss and the radiative heat flux obtained for the four test cases by the DOM and MC solutions with the SLW model. The application of the model follows the formulation described in Section 2.3; all remaining parameters necessary for the model follow Solovjov *et al.*, 2018a, with the gas absorption cross-section has been divided into twenty-five suplementar cross-sections (which corresponds to $J = 25$) between an interval of 3×10^{-4} m^2/mol to 60 m^2/mol. A total number of bundles of 10^8 is again using for the MC method.

Just as for the MC-GG and MC-WSGG solutions, the solution obtained MC method coupled to the SLW model agrees very well to the DOM one. For Cases 1.b and 1.g, the relative deviations for the radiative heat flux at the walls does not exceed 4.0 %, whereas for Cases 2.b and 2.g the error in the maximum radiation loss within the medium is about 2.0 %.

3.4 Sensibility to the number of energy bundles

Before concluding, it is worth a brief comment on the sensibility of the MC solution to the number of energy bundles. To illustrate this, consider Fig. 5, that shows the processing time required by the MC method and the error associated to this solution as a function of the total number of bundles for $10^4 \leq N_b \leq 10^8$. For convenience, the computational time required by the MC solution, t_{MC}, is shown in the figure in dimensionless form dividing it by the computational time associated to the DOM solution, t_{DOM}. The error of the MC method is quantified by the deviation, relative to the DOM result, for the radiative heat flux at the wall, but deviations in other quantities or other positions lead to similar conclusions.

As N_b increase, there is a corresponding increase in the time required for the solution with the Monte Carlo method. In fact, when applied alongside either the GG or WSGG models, t_{MC}/t_{DOM} increases almost linearly with N_b; this is to be expected, since the computational cost of the solution is directly related to the number of bundles that must be tracked from their emission to their absorption. The N_b-t_{MC}/t_{DOM} relation when the SLW model is employed is also approximately linear for $N_b > 10^6$. For smaller N_b, the cost of processing all the bundles for the MC-SLW solution or of solving the radiative transfer equation for the MC-DOM solution gets comparable to the cost of calculating κ_j and a_j for that model, which brings t_{MC} and t_{DOM} closer together. If a more efficient method for computing the gray gas coefficients were used, such as a rank transmutation for applying the rank-correlated method (Webb *et al.*, 2019), the linear N_b-t_{MC}/t_{DOM} relation for the MC-SLW solution would likely extend to smaller N_b.

Furthermore, note that, although the t_{MC}/t_{DOM} ratio is the largest for the GG model, this does not mean that this model entails the large computational cost among the ones tested—in fact, the true conclusion from the t_{MC}/t_{DOM} plot is exactly

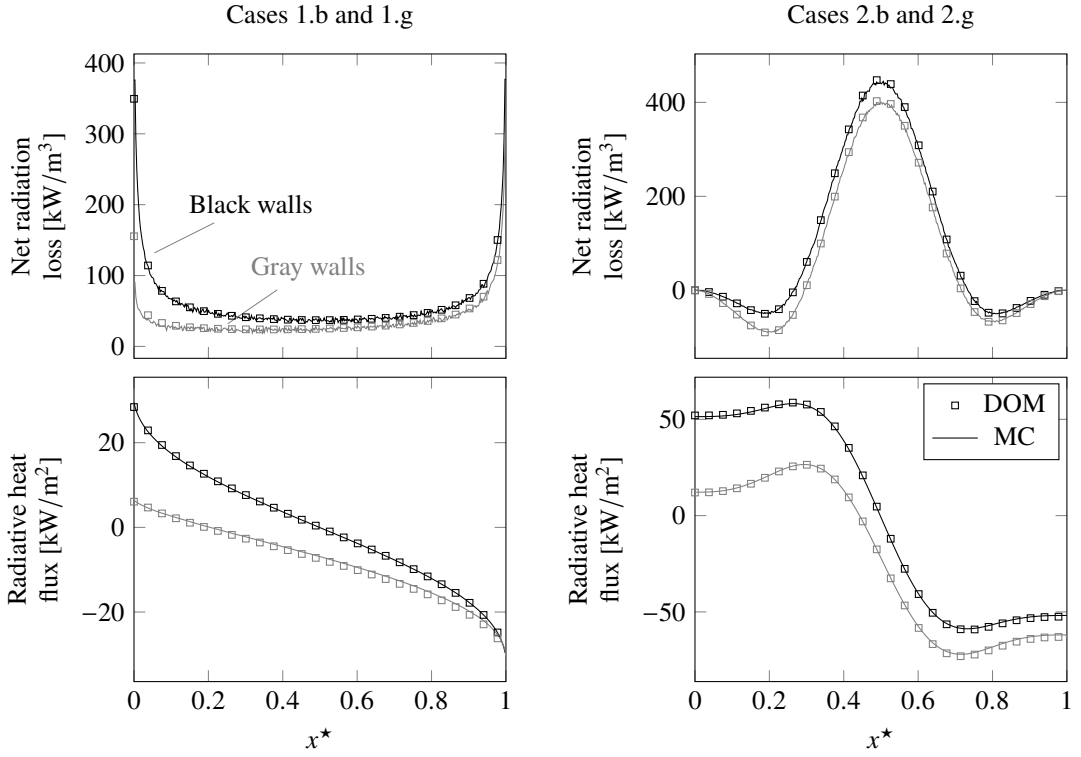

Figure 4. Comparison between the results of the DOM and of the MC method for the SLW model

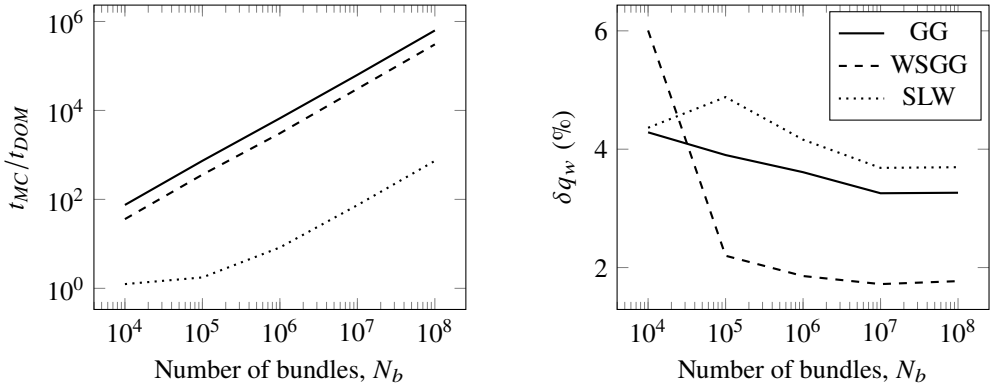

Figure 5. Ratio between the processing time necessary for the MC and DOM solutions (left) and difference in the wall radiative heat flux between the two solution (right) as a function of the total number of bundles used for the MC method. Results for Case 1.b

the opposite of this. When applying the GG model with the DOM, the RTE needs only be solved a single time for each optical path; for the WSGG or SLW models, on the other hand, the RTE must be solved $J + 1$ times, so, at least in the framework of the DOM, the computational cost of these models are larger than that of the GG model (and, because the total number of gray gases is larger for the SLW than for the WSGG model, t_{DOM} is larger for the former). However, for the MC method, the computational cost is related to the total number of bundles, which is the same for any one of the spectral models, si the values of t_{MC} for the GG, WSGG and SLW models are comparable. This is why t_{MC}/t_{DOM} is the largest for the solution with the GG model and smallest for the SLW one.

As expected, the accuracy of the MC method increases with increasing N_b, although starting from $N_b = 10^6$ the differences relative to the DOM are at most 4 % regardless of the spectral model. However, with $N_b = 10^6$ the spatial distribution of the results within the medium still shows visible oscillations, particularly for the radiation loss. It is also interesting to note that the differences between MC and DOM solutions are smaller for the WSGG model. This has been verified for all cases, and is likely because the gray gases that compose that model span a wide range of gray gas absorption coefficient values, each then having significantly different importance for the overall radiative emission; therefore, the randomness in the selection of by which gray gases any given bundle is emitted makes the most important gas (i.e., the one with the largest $\kappa_j a_j$) be the one that emits the largest amount of bundles. The same effect is not as significant for the

SLW model due to the larger number of gray gases in this model.

While they have been omitted here for the sake of brevity, plots similar to Fig. 5 for the other test cases show the same general trend as to what has been discussed here. A difference worth noting is that, for the cases with gray walls (Cases 1.g and 2.g) the t_{MC}/t_{DOM} ratio is smaller than that of the cases with black walls (i.e., the MC method, although still more expensive than the DOM, is more computationally efficient). This occurs because, whenever $\varepsilon_w \neq 1$, the solution of the RTE entails an iterative procedure, which is not required by the Monte Carlo method.

4. CONCLUSIONS

This paper reports the development and validation of a Monte Carlo solver for the radiative tranfer problem in a one-dimensional medium slab employing different spectral gas models, which is part of an ongoing research on the application of MC methods in radiative transfer problems. The method was implemented as a Fortran code and is capable for solving the radiative transfer problem for homogeneous and non-homogeneous media subjected to isothermal or non-isothermal conditions and bounded by black or gray walls. Three widely used spectral models were coupled to the MC method: the gray gas, the weighted-sum-of-gray gases, and the spectral line-based WSGG models.

Through comparisons with results obtained by the solution of the radiative transfer equation using a discrete ordinates method, which was carried out in a well-established in-house code, the implementations were validated for a set of test cases. The resulting spatial distributions of the net radiation loss and radiative heat flux showed a remarkable agreement for the two solutions, regardless of the spectral model used, attesting that the MC method was implemented successfully.

5. ACKNOWLEDGMENTS

Author FHRF thanks CNPq for research grant 302686/2017-7.

6. REFERENCES

Cassol, F., Brittes, R., Centeno, F.R., da Silva, C.V. and França, F.H.R., 2015. "Evaluation of the gray gas model to compute radiative transfer in non-isothermal, non-homogeneous participating medium containing CO_2, H_2O and soot". *Journal of the Brazilian Society of Mechanical Sciences and Engineering*, Vol. 37, No. 1, pp. 163–172. doi:10.1007/s40430-014-0168-5.

Cherkaoui, M., Dufresne, J.L., Fournier, R., Grandpeix, J.Y. and Lahellec, A., 1996. "Monte Carlo simulation of radiation in gases with a narrow-band model and a net-exchange formulation". *Journal of Heat Transfer*, Vol. 118, No. 2, pp. 401–407. doi:10.1115/1.2825858.

Cherkaoui, M., Dufresne, J.L., Fournier, R., Grandpeix, J.Y. and Lahellec, A., 1998. "Radiative net exchange formulation within one-dimensional gas enclosures with reflective surfaces". *Journal of Heat Transfer*, Vol. 120, No. 1, pp. 275–278. doi:10.1115/1.2830053.

Denison, M. and Webb, B., 1993. "An absorption-line blackbody distribution function for efficient calculation of total gas radiative transfer". *Journal of Quantitative Spectroscopy and Radiative Transfer*, Vol. 50, No. 5, pp. 499–510. doi:10.1016/0022-4073(93)90043-h.

Dorigon, L.J., Duciak, G., Brittes, R., Cassol, F., Galarça, M. and França, F.H.R., 2013. "WSGG correlations based on HITEMP2010 for computation of thermal radiation in non-isothermal, non-homogeneous H_2O/CO_2 mixtures". *International Journal of Heat and Mass Transfer*, Vol. 64, pp. 863–873. doi:10.1016/j.ijheatmasstransfer.2013.05.010.

Fleck, J.J., 1961. "The calculation of nonlinear radiation transport by a Monte Carlo method". Technical report. doi:10.2172/4466389.

Fonseca, R.J.C., Fraga, G.C., da Silva, R.B. and França, F.H.R., 2018. "Application of the WSGG model to solve the radiative transfer in gaseous systems with nongray boundaries". *Journal of Heat Transfer*, Vol. 140, No. 5, p. 052701. doi:10.1115/1.4038548.

Fraga, G., Zannoni, L., Centeno, F. and França, F., 2019. "Evaluation of different gray gas formulations against line-by-line calculations in two- and three-dimensional configurations for participating media composed by CO_2, H_2O and soot". *Fire Safety Journal*, Vol. 108, p. 102843. doi:10.1016/j.firesaf.2019.102843.

Haji-Sheikh, A. and Howell, J.R., 2006. "Monte Carlo methods". In *Handbook of Numerical Heat Transfer*, John Wiley & Sons, Inc., pp. 249–295. doi:10.1002/9780470172599.ch8.

Howell, J.R., 1998. "The Monte Carlo method in radiative heat transfer". *Journal of Heat Transfer*, Vol. 120, No. 3, pp. 547–560. doi:10.1115/1.2824310.

Howell, J.R. and Perlmutter, M., 1964a. "Monte Carlo solution of thermal transfer through radiant media between gray walls". *Journal of Heat Transfer*, Vol. 86, No. 1, pp. 116–122. doi:10.1115/1.3687044.

Howell, J.R., Mengüç, M.P. and Siegel, R., 2016. *Thermal Radiation Heat Transfer*. CRC press, 6th edition.

Howell, J.R. and Perlmutter, M., 1964b. "Monte Carlo solution of radiant heat transfer in a nongrey nonisothermal gas with temperature dependent properties". *AIChE Journal*, Vol. 10, No. 4, pp. 562–567. doi:10.1002/aic.690100429.

Lathrop, K.D. and Carlson, B.G., 1964. "Discrete ordinates angular quadrature of the neutron transport equation". Technical report. doi:10.2172/4666281.

Modest, M.F., 1978. "Three-dimensional radiative exchange factos for nongray, nondiffuse surfaces". *Numerical Heat Transfer*, Vol. 1, No. 3, pp. 403–416. doi:10.1080/10407787808913385.

Modest, M. and Poon, S., 1961. "Determination of three-dimensional radiative exchange factors for the space shuttle by Monte Carlo". Technical report.

Modest, M.F., 1991. "The weighted-sum-of-gray-gases model for arbitrary solution methods in radiative transfer". *Journal of heat transfer*, Vol. 113, No. 3, pp. 650–656. doi:10.1115/1.2910614.

Modest, M.F., 2013. *Radiative Heat Transfer*. Academic Press.

Perlmutter, M. and Howell, J.R., 1964. "Radiant transfer through a gray gas between concentric cylinders using Monte Carlo". *Journal of Heat Transfer*, Vol. 86, No. 2, pp. 169–179. doi:10.1115/1.3687090.

Solovjov, V.P., Andre, F., Lemonnier, D. and Webb, B.W., 2018a. "The scaled SLW model of gas radiation in non-uniform media based on planck-weighted moments of gas absorption cross-section". *Journal of Quantitative Spectroscopy and Radiative Transfer*, Vol. 206, pp. 198–212. doi:10.1016/j.jqsrt.2017.11.012.

Solovjov, V.P. and Webb, B.W., 2000. "An efficient method for modeling radiative transfer in multicomponent gas mixtures with soot". *Journal of Heat Transfer*, Vol. 123, No. 3, pp. 450–457. doi:10.1115/1.1350824.

Solovjov, V.P., Webb, B.W. and Andre, F., 2018b. "The rank correlated FSK model for prediction of gas radiation in non-uniform media, and its relationship to the rank correlated SLW model". *Journal of Quantitative Spectroscopy and Radiative Transfer*, Vol. 214, pp. 120–132. doi:10.1016/j.jqsrt.2018.04.026.

Tang, K.C. and Brewster, M.Q., 1999. "Analysis of molecular gas radiation: Real gas property effects". *Journal of Thermophysics and Heat Transfer*, Vol. 13, No. 4, pp. 460–466. doi:10.2514/2.6484.

Wang, A. and Modest, M.F., 2006. "Photon monte carlo simulation for radiative transfer in gaseous media represented by discrete particle fields". *Journal of Heat Transfer*, Vol. 128, No. 10, pp. 1041–1049. doi:10.1115/1.2345431.

Wang, A. and Modest, M.F., 2007a. "An adaptive emission model for monte carlo simulations in highly inhomogeneous media represented by stochastic particle fields". *Journal of Quantitative Spectroscopy and Radiative Transfer*, Vol. 104, No. 2, pp. 288–296. doi:10.1016/j.jqsrt.2006.07.023.

Wang, A. and Modest, M.F., 2007b. "Spectral monte carlo models for nongray radiation analyses in inhomogeneous participating media". *International Journal of Heat and Mass Transfer*, Vol. 50, No. 19-20, pp. 3877–3889. ISSN 00179310.

Webb, B.W., Solovjov, V.P. and André, F., 2019. "The spectral line weighted-sum-of-gray-gases (SLW) model for prediction of radiative transfer in molecular gases". In *Advances in Heat Transfer*, Elsevier, pp. 207–298. doi:10.1016/bs.aiht.2019.08.003.

7. RESPONSIBILITY NOTICE

The authors are solely responsible for the printed material included in this paper.